

Final report on the project entitled “Development of new theoretical and experimental methods for describing the collective properties of dislocations“

An in-depth understanding of the plastic response of crystalline materials on multiple scales, ranging from macroscopic sizes down to the atomic resolution, is vital for developing new materials. Although the properties of individual dislocations, the elementary carriers of plastic flow, has been long described to sufficient detail, many open issues related to the collective motion of these line-like defects still persist. The main objective of the work carried out in the project was the experimental and theoretical investigation of the statistical properties of the deformation of micron sized objects. The research carried out can be separated into seven different tasks.

1 DISLOCATION PATTERN FORMATION

Upon loading, dislocations self-organize into distinctive patterns of different kind, depending on the loading conditions. Although during the past decades several phenomenological models were proposed it is difficult to see how these models are related to the rather specific properties of dislocations (like long range scale free interactions, motion on well defined slip planes, or different types of short-range effects, etc.) they have to be considered as attempts to reproduce some phenomenological aspects of the patterns based on heuristic analogies. Already more than 20 years ago for the simplest possible dislocation configuration corresponding to 2D single slip, by a systematic coarse coarse-graining of the equations of motions of dislocations the PI and his coworkers derived a continuum theory on a systematic manner. In 2016 the theory has been generalized by the PI and his coworkers. By the linear stability analysis of the new theory it was shown that it is able to predict dislocation patterning, so it is the first continuum theory of patterning that is directly linked to the properties of individual dislocations. Since, however, linear stability analysis is not able to say anything about the global stability of the patterning the strongly nonlinear partial differential equations have been solved numerically with an appropriate finite element method. A clear patterning is observed with a characteristic length scale that is in good agreement with the one obtained by linear stability analysis. Moreover, it is found that the patterning is independent of the form of the initial perturbation added to the homogeneous initial dislocation distribution (see Fig. 1), meaning the patterning process is a general feature of the model.

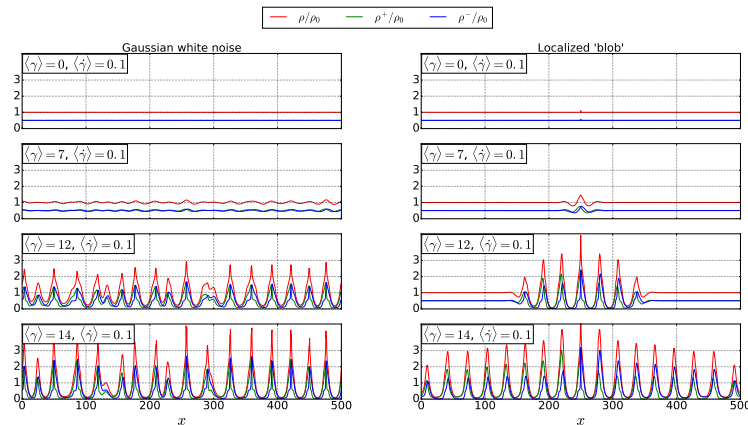


FIG. 1: Spatio-temporal evolution of dislocation density patterns for two different initial conditions; left: small Gaussian white noise superimposed on a homogeneous density distribution, right: localized density fluctuation superimposed on a homogeneous distribution.

Although the continuum theory is derived with a systematic coarse-graining procedure it is important to directly compare its predictions with discrete dislocation dynamics (DDD) simulations. In order to investigate this issue we have performed several 2D large scale DDD simulations under different loading conditions. To solve the continuum equations on an efficient way we have applied an extremal dynamics.

It is based on the rather fundamental feature of the continuum theory that the functional

$$P = \int \left[-\frac{1-\nu}{4\mu} (\Delta\chi)^2 + b\chi\partial_y\kappa + Gb^2A\rho \ln\left(\frac{\rho}{\rho_0}\right) + \frac{Gb^2D}{2} \frac{\kappa^2}{\rho} \right] d^2r \quad (1)$$

called plastic potential cannot increase during the evolution of the system. In $P(\rho, \kappa)$ ρ is the total, κ is the signed (so called geometrically necessary) dislocation densities, μ , ν and G are elastic constants, b is the Burgers vector, and χ is the stress function fulfilling the equilibrium condition $\delta P/\delta\chi = 0$. The two constants A and D are determined by the dislocation-dislocation correlation functions. Another key feature of the evolution of the dislocation system, we have to take into account, is if the external stress is lower then the flow stress proportional to $\sqrt{\rho}$ the dislocations do not move.

In the implementation suggested, densities are discretized on a regular grid of cell size a , and the flow stress τ_f is replaced by a local stochastic variable (representing the fluctuations of the underlying dislocation microstructure at every cell). For the distribution of the flow stress, in accordance with recent DDD results, a Weibull distribution is used. At every timestep, dislocation activity takes place at the site where decrease in P is the largest and it consists of a quantum of dislocation flux $\Delta\rho = a^{-2}$ (of either positive or negative dislocations) flowing through the cell boundary. If no such cell exists, the external stress is increased until one cell is triggered. This model is referred to as stochastic continuum dislocation dynamics (SCDD).

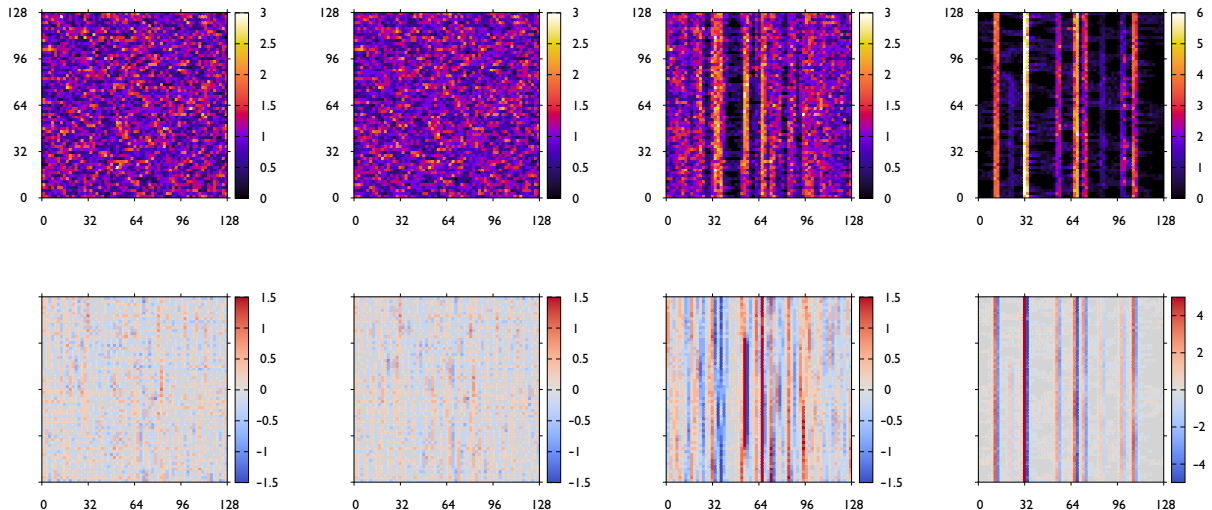


FIG. 2: Dislocation pattern evolution in SCDD simulations. Total and GND density maps obtained at different strain values.

As it is seen in Fig. 2. dislocation patterning develops in the SCDD model. The characteristic length scale emerges is in agreement with the prediction of the linear stability analysis. Moreover it is possible to directly compare the dislocation-dislocation correlation function obtained by DDD and SCDD. It is found that at appropriate parameter values the correlation functions obtained by the two methods show similar feature. Two papers in PRB were published on this issue.

It should be noted that unlike in many other physical system here the patterning is not related to a double-well shaped energy functional, the plastic potential is convex. Patterning is the result of the $\sqrt{\rho}$ dependence of the flow stress and the so called "gradient" terms related to the last two terms in the plastic potential (for more details see below). This is a completely new interpretation of dislocation patterning.

2 CONTINUUM THEORY OF CURVED DISLOCATIONS

The continuum theory discussed above corresponds to a rather idealized 2D configuration containing straight parallel edge dislocations. Although it is able to account for several important features of dislocation systems, like patterning, or size effect, it certainly cannot be considered as the "final" theory of

dislocation evolution on the continuum level. The curvature of dislocations is important to model many aspects of the evolution of the dislocation system. Although in the original work plan of the project we did not plan to work on this problem, during the course of the project we were able to make an important step in the generalization of the 2D theory for curved dislocations. In order to start explaining the main idea of the generalization let us start with the evolution equation of the 2D system:

$$\partial_t \rho = \partial_x \left\{ \kappa M_0 \partial_x \frac{\delta P}{\delta \kappa} + \rho M_0 \partial_x \frac{\delta P}{\delta \rho} \right\}, \quad (2)$$

$$\partial_t \kappa = \partial_x \left\{ \rho M_0 \zeta \left(\partial_x \frac{\delta P}{\delta \kappa} \right) + \kappa M_0 \partial_x \frac{\delta P}{\delta \rho} \right\} \quad (3)$$

where P is the plastic potential given above and $\zeta(\tau^*)$ is a on-off type mobility function shown in Fig. 3, where $\tau^* = \partial_x(\delta P/\delta \kappa)$ and τ^y is the yield stress. As it is seen if the GND density $\kappa = 0$ the mobility is

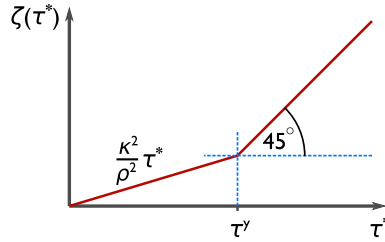


FIG. 3: The $\zeta(\tau^*)$ mobility function.

zero below the yield stress. With a long but straightforward calculation one can see that the above form ensures that the plastic potential cannot increase during the evolution of the system.

For the kinematics of the evolution of the dislocation system recently Thomas Hochrainer and his coworkers suggested an elegant method. The key step is to extend the problem into a higher dimension. For a dislocation loop in a plane they introduced an extra dimension corresponding to the angle φ of the tangent vector of the loop. In this (2+1)D the loop is constructed so that the x and y components of the tangent vector of the "new" loop are equal to the corresponding x and y component of the tangent vector of the "original" loop, while the third component is equal to the curvature of the 2D loop (see

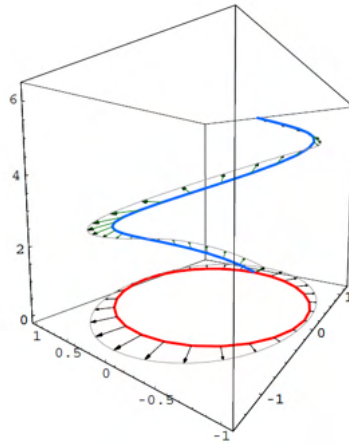


FIG. 4: The 3D mapping of the dislocation loop.

Fig 4). This is a unique mapping. With this the kinematics of the system is described by 3 fields, the generalized dislocation density $\rho'(\vec{r}, \varphi, t)$, the generalized curvature field $q'(\vec{r}, \varphi, t)$ and the scalar velocity field $v'(\vec{r}, \varphi, t)$.

By applying appropriate Lie derivation the evolution of the fields ρ' and q' are formulated so that the curve remain continuous. So, it does not end in the 3D volume considered (for details see [1] "Dynamics of curved dislocation ensembles, I. Groma, PD. Ispánovity, T. Hochrainer, PRB, 103 (17), 174101, (2021)").

To get a closed theory, however, one should give how the velocity field v' depends on ρ' and q' . For that first we proposed to reduce the degree of freedom of the problem. Namely, the $\rho'(\vec{r}, \varphi, t)$, $q'(\vec{r}, \varphi, t)$, and $v'(\vec{r}, \varphi, t)$ fields are periodic functions of the angle φ so they can be expanded into a Fourier series. As a simplest possible approximation that can account for stored and GND dislocations we stopped at the second Fourier terms, i.e. we took the forms:

$$\rho'(\mathbf{r}, \varphi) \approx \rho(\mathbf{r}) + 2 \cos \varphi \kappa_1(\mathbf{r}) + 2 \sin \varphi \kappa_2(\mathbf{r}), \quad (4)$$

$$v'(\mathbf{r}, \varphi) \approx v^m(\mathbf{r}) + \cos \varphi v_1^d(\mathbf{r}) + \sin \varphi v_2^d(\mathbf{r}), \quad (5)$$

$$q'(\mathbf{r}, \varphi) \approx q(\mathbf{r}) + \cos \varphi Q_2(\mathbf{r}) - \sin \varphi Q_1(\mathbf{r}). \quad (6)$$

After substituting these forms into the evolution equation and carrying out appropriate integration for φ we have got evolution equations for the fields $\rho(\mathbf{r}, t)$, $\kappa_1(\mathbf{r}, t)$, $\kappa_2(\mathbf{r}, t)$, and $q(\mathbf{r}, t)$ (for details see [1]). (One can find that the fields $Q_1(\mathbf{r}, t)$, $Q_2(\mathbf{r}, t)$ are directly related to $\rho(\mathbf{r}, t)$.)

This is, however, still the kinematics of the problem because the velocity fields $v^m(\mathbf{r})$, $v_1^d(\mathbf{r})$, $v_2^d(\mathbf{r})$ are not known. To get a closed theory they had to be given as a function of the $\rho(\mathbf{r}, t)$, $\kappa_1(\mathbf{r}, t)$, $\kappa_2(\mathbf{r}, t)$, and $q(\mathbf{r}, t)$ fields. In order to get these relations, like for the straight parallel dislocation problem, we have assumed that there is a scalar functional of the relevant fields $P(\rho(\mathbf{r}, t), \kappa_1(\mathbf{r}, t), \kappa_2(\mathbf{r}, t), q(\mathbf{r}, t))$ that cannot increase during the evolution of the system. Like in irreversible thermodynamics independently of the actual form of P this impose a rather strong restrictions on the possible relations. Taking the simplest possible forms we proposed the evolution equations summarized in Fig.5. The plastic potential suggested

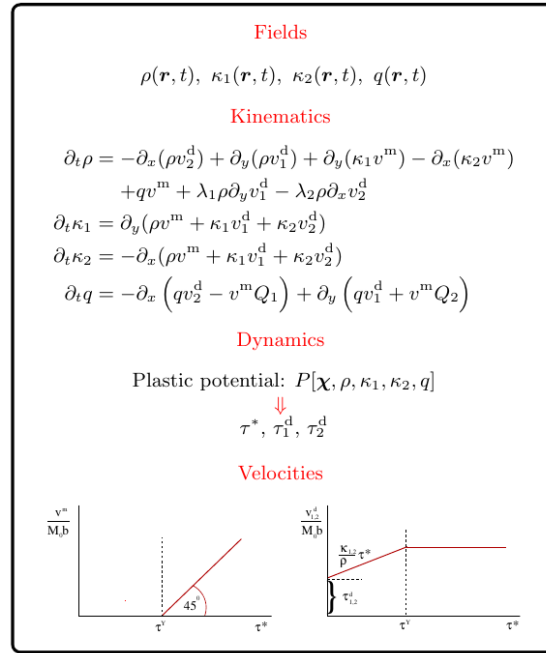


FIG. 5: Summary of the model

is a natural generalization of the 2D one given above, and the stress "like" variables τ_1^d , τ_2^d , and τ^* are proportional to the gradient of the different functional derivatives of P (see [1]).

The continuum model suggested has to be validated by DDD simulation, that is an important project for the near future, but we believe this is the first continuum theory of curved dislocations that is derived on a systematic manner.

3 NANODEFORMATION STAGE

In order to carry out the nanodeformation experiments planned we had to further develop our custom made nanodeformation stage (see Fig. 6) that is able to move the sample in 3 direction with nanometer precision, while the load is measured with a few μN precision. The device can be placed inside a scanning electron microscope (SEM).

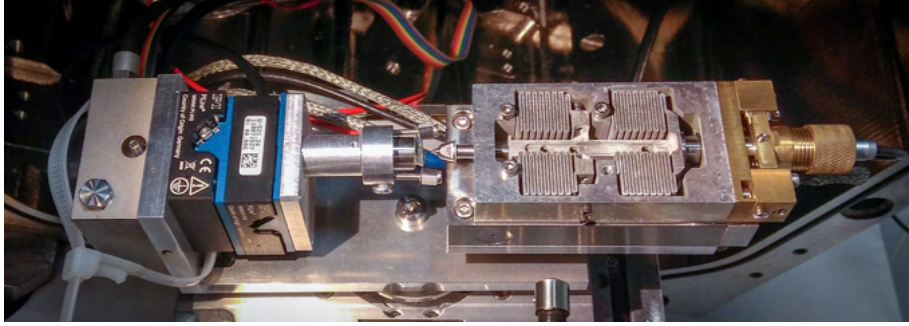


FIG. 6: The nanodeformation stage

Moreover, an unique feature of the device is that an acoustic emission detector is also built in making possible to detect the acoustic emission (AE) signal generated during the deformation. It should be noted that the AE signal is generated in a rather small volume (about $100\mu\text{m}^3$) resulting that its detection is a nontrivial task.

To improve the performance of the device, during the course of the project, we redesigned and rebuilt a considerable part of the controlling electronics. Moreover a completely new controlling software was developed. So, with the current setup our custom made nanodeformation stage allows us to collect three different types of information simultaneously during compression of the micropillars: (i) stress and strain, (ii) acoustic signal from a piezoelectric transducer and (iii) visual images using the electron beam of the SEM.

4 DISLOCATION AVALANCHES

With our unique experimental set-up, which detects the weak AE waves of dislocation slip, we have performed compression tests on Zn micropillars. A typical deformation morphology can be seen in Fig. 7. The deformation consists of random spatially strongly localized avalanche corresponding to collective dislocation motions. The dislocation avalanches are accompanied with stress drops and large AE signals (see Fig.5).

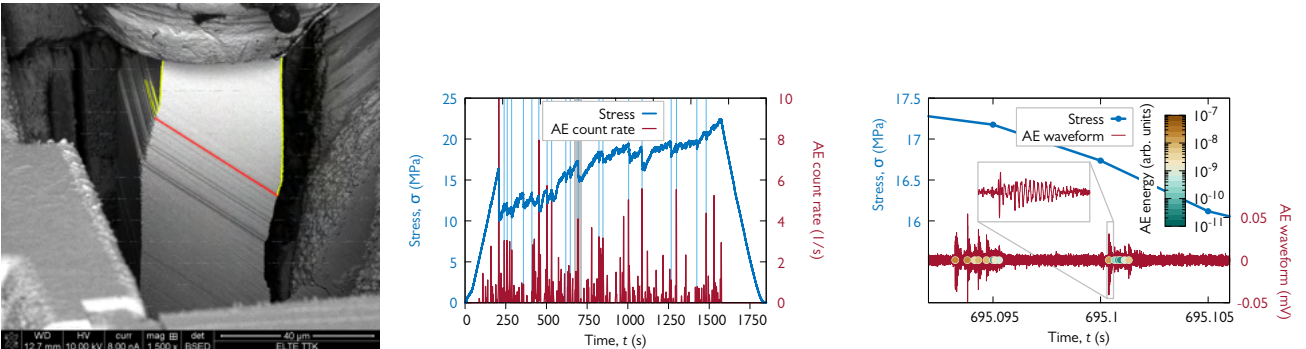


FIG. 7: Compressed pillar morphology, Stress-time and acoustic emission signal, Enlarged stress-time and acoustic emission signal.

According to our detailed analysis there is a strong correlation between the height of the stress drops and the energy emitted in AE signal. The AE data also reveal a surprising two-level structure of plastic events,

which otherwise appear as a single stress drop. Hence, our experiments unravel the missing relationship between the properties of acoustic signals and the corresponding local deformation events.

To quantify the statistical properties of the stress drops and the AE signals a detailed analysis of the measured data was performed. In agreement with studies on other single crystalline micropillars the distribution of the size of the individual stress drops follows a scale-free distribution with a cut-off

$$P(\Delta\sigma) \propto \Delta\sigma^{-\alpha_\sigma} \exp\left(-\frac{\Delta\sigma}{\sigma_0}\right). \quad (7)$$

If the axes are re-scaled with the cross section $A = d^2$ of the micropillars (that is, force drop $\Delta F = A\Delta\sigma$ is considered as variable) the curves corresponding to different pillar size overlap and can be fitted with a master function yielding $\alpha_\sigma = 1 : 8 \pm 0 : 1$ and $F_0 = 1 : 5 \pm 0 : 1 mN$ for the exponent and the cutoff, respectively. The distribution of the AE event energy E is characterized by another scale-free distribution now without an apparent cut-off and dependence on pillar size:

$$P(E) \propto E^{-\alpha_E} \quad (8)$$

with $\alpha_E = 1.7 \pm 0.1$.

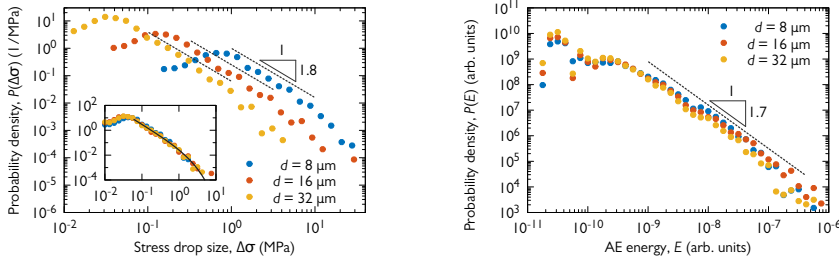


FIG. 8: Stress drop and AE energy statistic.

A remarkable feature of the AE signals observed is that the main shock is followed by a series of aftershocks. It is found that the rate of aftershocks is inversely proportional to the time elapsed after the main shock. This is in accordance with the aftershock statistic observed for earthquake (Omori law).

The results obtained indicate that despite the fundamental differences in deformation mechanism and involved length- and time-scales, dislocation avalanches and earthquakes are essentially alike. On the results obtained a paper entitled "Dislocation Avalanches: Earthquakes on the Micron Scale" is accepted for publication in Nature Communications.

5 TWINNING IN MAGNESIUM MICROPILLARS

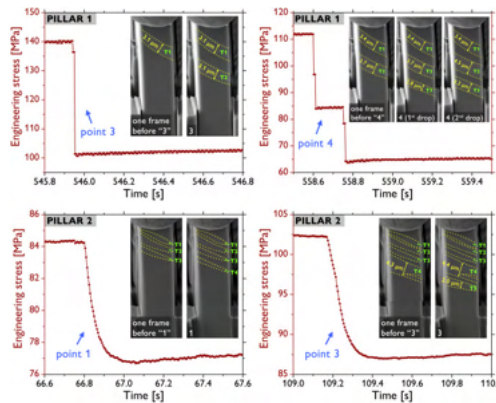


FIG. 9: Twinning in magnesium micropillars.

In magnesium beside dislocation motion twinning is a key mechanism of plastic deformation. For the first time we could detect twin nucleation and grows in compressed magnesium micropillars. The twin nucleation is also accomplished with a significant stress drop and a strong AE signal. We could analyze the twin growth rate as a function of the mode and the level of deformation. The results obtained was published in a paper entitled "On the dynamics of twinning in magnesium micropillars" in Materials & Design.

6 HR-EBSD INVESTIGATIONS

EBSD is a powerful well established method to determine the local orientation of crystalline materials with a spatial resolution of about $10\mu m$. With the traditionally applied analysis of the EBSD Kikuchy patterns the orientation can be determined by about 0.1° resolution. Recently at the Oxford University Wilkinson and coworkers suggested that by the detailed cross correlation analysis of the EBSD patterns obtained from a reference and another point the relative strain (more precisely the distortion tensor) and stress states of the two point can be determined. Knowing the distortion tensor β_{ij} the $i3$ components of the dislocation density tensor

$$\alpha_{i3} = \partial_1\beta_{i2} - \partial_2\beta_{i1} \quad (9)$$

can also be determined. (Since the distortion is measured only on the surface the other components of α_{ij} depending on the ∂_3 derivatives cannot be determined.) The scalar quantity defined as

$$\rho_{GND} = \frac{1}{b} \sqrt{\alpha_{13}^2 + \alpha_{23}^2 + \alpha_{33}^2} \quad (10)$$

is a characteristic quantity measuring the local "net" Burgers vector (called GND density).

Moreover according to an earlier theoretical result of the PI the dislocation density can be determined from the tail of the internal stress probability distribution. So, beside X-ray line profile analysis HR-EBSD offers a new method to determine the dislocation density.

In order to see the dislocation microstructure developing in compressed Cu micropillars we have determined the internal stress and ρ_{GND} maps by HR-EBSD. What was completely new in our investigations is that by FIB we removed surface sections of the pillars in several steps and repeated the HR-EBSD measurement on the "new" surfaces. The method makes possible the get a 3D map of the stress and the GND. Typical result can be seen in Fig. 10. As it is seen like in bulk deformed Cu crystal (see below)

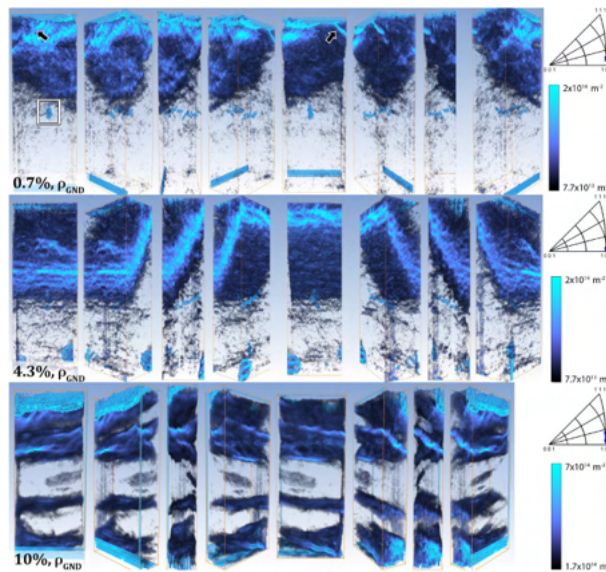


FIG. 10: 3D models of GND density values for the three micropillars (top row: 0.7%, middle row: 4.3%, bottom row: 10%) rotated around for inspection.

regions with large dislocation density (called dislocation wall) develop in micropillars too. The results obtained was published in a paper entitled "Investigation of geometrically necessary dislocation structures in compressed Cu micropillars by 3-dimensional HR-EBSD" in MSE.

7 FRACTAL STRUCTURE OF DISLOCATION PATTERNS

It is known for several decades that dislocations tend to form different patterns. It was found by detailed TEM investigation that in Cu single crystals oriented for ideal multiple slip a scale free cell like structure is formed with a fractal dimension of about 2.8. Since with EBSD we can scan about 10 times larger area than by TEM the new HR-EBSD method offers a unique method for a detailed fractal analysis of the dislocation microstructure.

During the project we have performed x-ray line profile analysis and HR-EBSD investigations on Cu single crystals deformed up to different stress levels. From the analysis of the tail of the x-ray line profile one can determine the relative spatial fluctuation $\sigma = \langle \rho^2 \rangle / \langle \rho \rangle^2$. According to our results while the dislocation density increases monotonically with the deformation level, σ shows a sharp maximum at a given stress level (see Fig. 11). The GND maps obtained by HR-EBSD is seen in Fig. 12. It should be

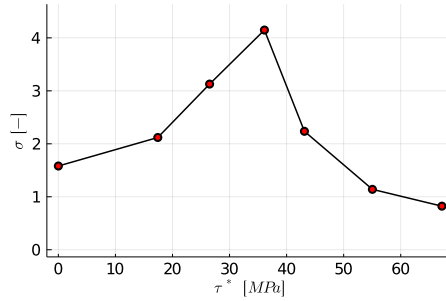


FIG. 11: Relative average dislocation density fluctuation versus stress level.

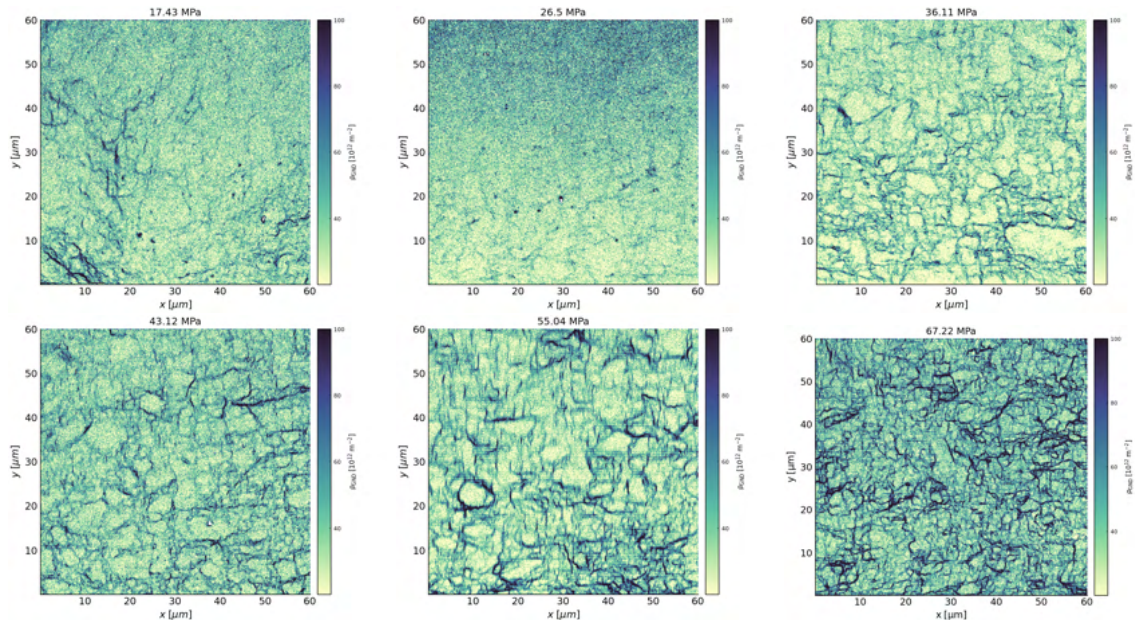


FIG. 12: GND maps at different stress levels.

noted dislocation cell structure was not detected by HR-EBSD earlier.

After applying a newly developed "cleaning" method allowing to remove the "separate" black points in the maps the fractal dimension of the cell structure could be determined. We have found that the fractal

dimension is a monotonic function of relative dislocation fluctuation σ . It decreases with increasing relative dislocation fluctuation.

Although at the moment we do not have a theoretical explanation only for periodic dislocation patterning observed at periodic loading, the results obtained are important for further dislocation patterning models. A paper is being prepared on these results.